

Recovery of the time-dependent source term in the stochastic fractional diffusion equation with heterogeneous medium

Shubin Fu^{*1} and Zhidong Zhang^{†2}

¹Department of Mathematics, University of Wisconsin-Madison, USA

²Department of Mathematics and Statistics, University of Helsinki, Finland

January 6, 2022

Abstract

In this work, an inverse problem in the fractional diffusion equation with random source is considered. The measurements used are the statistical moments of the realizations of single point data $u(x_0, t, \omega)$. We build the representation of the solution u in integral sense, then prove that the unknowns can be bounded by the moments theoretically. For the numerical reconstruction, we establish an iterative algorithm with regularized Levenberg-Marquardt type and some numerical results generated from this algorithm are displayed. For the case of highly heterogeneous media, the Generalized Multiscale finite element method (GMsFEM) will be employed.

Keywords: inverse problem, fractional diffusion equation, random source, GMsFEM, regularized iterative algorithm.

AMS classification: 35R30, 35R11, 65C30, 65M32, 65M60.

1 Introduction

1.1 Mathematical statement

The mathematical model in this work is stated as follows:

$$\begin{cases} \partial_t^\alpha u + \mathcal{A}u = f(x)[g_1(t) + g_2(t)\dot{W}(t)] =: f(x)g(t, \omega), & (x, t) \in D \times (0, T], \\ u(x, t) = 0, & (x, t) \in \partial D \times (0, T], \\ u(x, 0) = 0, & x \in D. \end{cases} \quad (1)$$

^{*}shubinfu89@gmail.com

[†]zhidong.zhang@helsinki.fi

The domain $D \subset \mathbb{R}^d$, $d = 1, 2, 3$ has sufficiently smooth boundary, and ∂_t^α with $\alpha \in (1/2, 1)$ denotes the Djrbashyan-Caputo fractional derivative, defined as

$$\partial_t^\alpha \psi(t) = \frac{1}{\Gamma(1-\alpha)} \int_0^t (t-\tau)^{-\alpha} \psi'(\tau) d\tau,$$

where $\Gamma(\cdot)$ is the gamma function. The lower bound $\alpha > 1/2$ is set to ensure the well definedness of the Ito integral $I_t^\alpha g(t, \omega)$ and this can be seen in the next section. The operator $\mathcal{A} : H^2(D) \mapsto L^2(D)$ is an elliptic operator defined as $\mathcal{A}\psi(x) = -\nabla \cdot (\kappa(x)\nabla\psi(x))$, and $\kappa(x)$ may be highly heterogeneous. The source term $f(x)g(t, \omega) = f(x)[g_1(t) + g_2(t)\dot{\mathbb{W}}(t)]$ contains the targeted unknowns g_1, g_2 , while the spatial component $f(x)$ is given. $\dot{\mathbb{W}}(t)$ is the white noise derived from the Brownian motion and then $g(t, \omega) = g_1(t) + g_2(t)\dot{\mathbb{W}}(t)$ constitutes an Ito process, see [41] for details.

Our data is the moments of the realizations of u on a single point $x_0 \in D$ with the restriction $x_0 \notin \text{supp}(f)$, which is different from [31]. This condition will make the inverse problem more challenging in mathematics, but is meaningful in practical application. For instance, regarding equation (1) as the contaminant diffusion system, solution u will be the concentration of pollutant, and $\text{supp}(f)$ is the location of pollution source, in which it is severely polluted. If the pollutant is harmful for human body, it is not allowed to observe inside the support of f considering staff's health. Reflected on mathematics, we should set the restriction $x_0 \notin \text{supp}(f)$, even though it will increase the difficulty. Actually, given $x_0 \in \text{supp}(f)$, this inverse problem will be reduced to Volterra integral equations, and the stability result and iterative algorithm follow straightforwardly. See Remark 1 for details.

The precise mathematical description of this inverse problem is given as follows: observe $u(x_0, t, \omega)$, $x_0 \notin \text{supp}(f)$, then use the statistical moments of the measurements to reconstruct g_1, g_2 simultaneously.

1.2 Physical background and literature

In microscopic level, the random motion of a single particle can be viewed as a diffusion process. The classical diffusion equation can be deduced to describe the motion of particles, if we assume the key condition, the mean squared displacement of jumps after a long time is proportional to time, i.e. $\overline{(\Delta x)^2} \propto t$, $t \rightarrow \infty$. However, recently, people found some anomalous diffusion phenomena [5, 8, 17, 26], in which the assumption $\overline{(\Delta x)^2} \propto t$, $t \rightarrow \infty$ is violated. Sometimes it may possess the asymptotic behavior of t^α , i.e. $\overline{(\Delta x)^2} \propto t^\alpha$, $\alpha \neq 1$. The different rate will lead to a reformulation to the diffusion equation, introducing the time fractional derivative in it, and the corresponding equations are called fractional differential equations (FDEs). We list some applications of FDEs, to name a few, the thermal diffusion in media with fractal geometry [39], ion transport in column experiments [19], dispersion in a heterogeneous aquifer [1], non-Fickian diffusion in geological formations [6], the analysis on viscoelasticity in material science [35, 49]. [37] provides an extensive list.

If uncertainty is added in the source term, the FDE system will become more complicated and meaningful. Since it is common to meet a diffusion source, which is defined as a stochastic process to describe the uncertain character imposed by nature. As a consequence, it is worth to investigate the diffusion system with a random source. In such situation the solution u will be written as a stochastic process, which makes the analysis more challenging.

In addition, to deal with the case of highly heterogeneous medium $\kappa(x)$, the Generalized Multiscale Finite Element Method (GMsFEM [13]) will be used to simulate the forward problem of equation (1). The introduction of GMsFEM will be given in section 4.3.1.

For a comprehensive understanding of fractional calculus and FDEs, see [25, 45, 7] and the references therein. For inverse problems in FDEs, [24] is an extensive review. See [14, 50, 40] for inverse source and coefficient problems; see [22] for unique continuation principle; see [21] for Carleman estimate in FDEs; see [18, 27, 42] for fractional Calderon problem. Furthermore, if we extend the assumption $(\Delta x)^2 \propto t^\alpha$ to a more general case $(\Delta x)^2 \propto F(t)$, the multi-term fractional diffusion equations and even the distributed-order differential equations will be generated, [43, 47, 30, 29]. For numerical methods for inverse problems, see [4, 3] and the references therein. Literature about the GMsFEM and its applications can be found in [13, 12, 9, 11, 10].

1.3 Main result and outline

Throughout this paper, the following restrictions on spatial component f , observation point x_0 , and the unknowns g_1, g_2 are supposed to be valid.

Assumption 1.

- $g_l \in L^\infty(0, T)$, $l = 1, 2$, and set $M > 0$ such that $\|g_1\|_{L^\infty(0, T)} \leq M < \infty$;
- g_1 changes its sign N times on $(0, T)$ and $N < \infty$;
- $f \in H^2(D) \cap H_0^1(D)$ and $0 \leq f(x) \leq C_f < \infty$ for $x \in D$;
- $x_0 \notin \text{supp}(f)$, namely, $f(x_0) = 0$.

Now we can state the main result, which says the unknowns can be limited by some statistical moments of observations $u(x_0, t, \omega)$.

Theorem 1. Under Assumption 1, let $v(x, t)$ satisfy equation (6) and define

$$C_\alpha = 1/\Gamma(2 - \alpha), \quad B_\eta = \|v(x_0, \cdot)\|_{L^1(0, \eta)}^{-1}, \quad \eta > 0 \text{ be small.}$$

Then the following estimates for g_1 and g_2 are valid.

(a) If $N = 0$,

$$\|g_1\|_{L^1(0, T-\eta)} \leq C_\alpha B_\eta T^{1-\alpha} \mathbb{E}[\|u(x_0, \cdot, \omega)\|_{L^1(0, T)}].$$

(b) If $N > 0$,

$$\|g_1\|_{L^1(0,T-\eta)} \leq \frac{(B_\eta C_f T + 1)^{N+1} - 1}{B_\eta C_f T} \left(C_\alpha B_\eta T^{1-\alpha} \mathbb{E}[\|u(x_0, \cdot, \omega)\|_{L^1(0,T)}] + 2M\eta \right).$$

(c)

$$\|g_2\|_{L^2(0,T-\eta)} \leq \eta^{1/2} B_\eta \left\| \mathbb{V}[I_t^{1-\alpha} u(x_0, t, \omega)] \right\|_{L^1(0,T)}^{1/2}.$$

In this theorem, $I_t^{1-\alpha}$ means the fractional integral operator, and \mathbb{E}, \mathbb{V} are the notations for expectation and variance, respectively. These knowledge can be seen in section 2. Noting that the stochastic process $g_2(t)\dot{\mathbb{W}}(t)$ is independent of the sign of g_2 by the properties of \mathbb{W} in section 2, sequentially we consider g_2^2 instead of g_2 . That's why the L^2 norm of g_2 is estimated.

The remaining part of this manuscript is structured as follows. Section 2 includes the preliminaries, such as the probability space (Ω, \mathcal{F}, P) and the stochastic solution u for equation (1). Also, some auxiliary results like the reverse convolution inequality and the maximum principles in fractional diffusion equations are collected. In section 3, we prove Theorem 1. After that the numerical reconstruction for the unknowns is investigated in section 4. We construct the regularized Levenberg-Marquardt iteration (15), and prove its convergence—Proposition 2. Some numerical results generated by iteration (15) are also displayed. Furthermore, some brief knowledge of GMsFEM is provided in this section.

2 Preliminaries

2.1 Brownian motion and Ito isometry formula

To state the Ito formula, firstly we need to give the setting of probability space.

Definition 1. We call (Ω, \mathcal{F}, P) a probability space if Ω denotes the nonempty sample space, \mathcal{F} is the σ -algebra of Ω and $P : \mathcal{F} \mapsto [0, 1]$ is the probability measure.

With the above definition, the expectation \mathbb{E} and variance \mathbb{V} of a random variable X can be given as

$$\mathbb{E}[X] = \int_{\Omega} X(\omega) dP(\omega), \quad \mathbb{V}[X] = \mathbb{E}[(X - E[X])^2].$$

The Brownian motion $\mathbb{W}(t)$, which is also called Wiener process in mathematics, has the following properties,

- $\mathbb{W}(0) = 0$;

- $\mathbb{W}(t)$ has continuous paths;
- $\mathbb{W}(t)$ has independent increments and satisfies

$$\mathbb{W}(t) - \mathbb{W}(s) \sim \mathcal{N}(0, t - s), \quad 0 \leq s \leq t,$$

where \mathcal{N} is the normal distribution.

Now the essential tool, Ito isometry formula can be stated.

Lemma 1. ([41]). *Let (Ω, \mathcal{F}, P) be a probability space and $\psi : [0, \infty) \times \Omega \rightarrow \mathbb{R}$ satisfy the following properties.*

- (1) $(t, \omega) \rightarrow \psi(t, \omega)$ is $\mathcal{B} \times \mathcal{F}$ -measurable, where \mathcal{B} denotes the Borel σ -algebra on $[0, \infty)$;
- (2) $\psi(t, \omega)$ is \mathcal{F}_t -adapted;
- (3) $\mathbb{E}[\int_0^S \psi^2(t, \omega) dt] < \infty$ for some $S > 0$.

Then the Ito integral $\int_0^S \psi(t, \omega) d\mathbb{W}(t)$, where $d\mathbb{W}(t)$ denotes the random measure derived from \mathbb{W} , is well defined, and it follows that

$$\mathbb{E}\left[\left(\int_0^S \psi(t, \omega) d\mathbb{W}(t)\right)^2\right] = \mathbb{E}\left[\int_0^S \psi^2(t, \omega) dt\right].$$

2.2 Stochastic weak solution

The randomness from $\mathbb{W}(t)$ means that we can not differentiate u in t for each $\omega \in \Omega$. As a consequence, we will define the weak solution u of equation (1) in the integral sense.

Firstly, the fractional integral operator I_t^α and the corresponding Ito integral $I_t^\alpha g(t, \omega)$ are given.

Definition 2. *The fractional integral operator I_t^α , $\alpha \in (1/2, 1)$ is defined as*

$$I_t^\alpha \psi(t) = \Gamma(\alpha)^{-1} \int_0^t (t - \tau)^{\alpha-1} \psi(\tau) d\tau, \quad t > 0.$$

Then we define $I_t^\alpha g(t, \omega)$ as

$$I_t^\alpha g(t, \omega) = I_t^\alpha g_1(t) + \Gamma(\alpha)^{-1} \int_0^t (t - \tau)^{\alpha-1} g_2(\tau) d\mathbb{W}(\tau).$$

Now we explain the necessity of the restriction $\alpha \in (1/2, 1)$. For $t \in (0, \infty)$, from the conditions $\alpha \in (1/2, 1)$ and $\|g_2\|_{C(0, \infty)} \leq M$, we have $(t - \tau)^{\alpha-1} g_2(\tau)$ is square-integrable on $(0, t)$. Then Lemma 1 yields that the Ito integral $\int_0^t (t - \tau)^{\alpha-1} g_2(\tau) d\mathbb{W}(\tau)$ is well defined.

In addition, the direct calculation gives that

$$I_t^\alpha \partial_t^\alpha \psi(t) = \psi(t) - \psi(0),$$

which implies the next definition of the weak solution for equation (1).

Definition 3 (Stochastic weak solution). *The stochastic process $u(\cdot, t, \omega) : (0, T] \times \Omega \mapsto L^2(D)$ is called as a stochastic weak solution of equation (1) if for each $\psi \in H^2(D) \cap H_0^1(D)$ and $\omega \in \Omega$, it holds that*

$$\langle u(\cdot, t, \omega), \psi(\cdot) \rangle_{L^2(D)} + \langle I_t^\alpha \mathcal{A}u(\cdot, t, \omega), \psi(\cdot) \rangle_{L^2(D)} = I_t^\alpha g(t, \omega) \langle f(\cdot), \psi(\cdot) \rangle_{L^2(D)}, \quad t \in (0, T].$$

2.3 Auxiliary lemmas

Here we list some auxiliary lemmas which will be used later. First the reverse convolution inequality is given.

Lemma 2. ([33, Lemma 3.1]). *Let $0 \leq T_1 < T_2 < \infty$ and $\eta > 0$ be arbitrarily given. Suppose that $\varphi_1 \in L^1(T_1, T_2 + \eta)$, $\varphi_2 \in L^1(0, T_2 - T_1 + \eta)$ and $\varphi_2 \geq 0$ on $(0, T_2 - T_1 + \eta)$.*

(a) *If φ_1 keeps its sign on $(T_1, T_2 + \eta)$, then*

$$\|\varphi_1\|_{L^1(T_1, T_2)} \|\varphi_2\|_{L^1(0, \eta)} \leq \left\| \int_{T_1}^t \varphi_1(s) \varphi_2(t-s) ds \right\|_{L^1(T_1, T_2 + \eta)}. \quad (2)$$

(b) *If φ_1 only keeps its sign on (T_1, T_2) , then*

$$\begin{aligned} \|\varphi_1\|_{L^1(T_1, T_2)} \|\varphi_2\|_{L^1(0, \eta)} &\leq \left\| \int_{T_1}^t \varphi_1(s) \varphi_2(t-s) ds \right\|_{L^1(T_1, T_2 + \eta)} \\ &\quad + 2 \|\varphi_1\|_{L^1(T_2, T_2 + \eta)} \|\varphi_2\|_{L^1(0, \eta)}. \end{aligned} \quad (3)$$

The next lemmas are the maximum principles in FDEs.

Lemma 3. (Maximum principle, [34, Theorem 2]). *Fix $T \in (0, \infty)$, let ψ satisfy the following fractional diffusion equation*

$$\partial_t^\alpha \psi + \mathcal{A}\psi = F(x, t), \quad (x, t) \in D \times (0, T), \quad (4)$$

and define $\lambda_T = \partial D \times [0, T] \cup \overline{D} \times \{0\}$. If $F \leq 0$, then

$$\psi(x, t) \leq \max \left\{ 0, \max \{ \psi(x, t) : (x, t) \in \lambda_T \} \right\}, \quad (x, t) \in \overline{D} \times [0, T].$$

Lemma 4. (Strong maximum principle, [32, Theorem 1.1]). *We set ψ as the solution of equation (4) and let $F = 0$, $\psi(x, 0) \geq 0$, $\psi(x, 0) \not\equiv 0$, $\psi(x, t) = 0$ on $\partial D \times (0, T)$. Then for any $x_0 \in D$, the set $\{t > 0 : \psi(x_0, t) \leq 0\}$ is at most a finite set.*

In addition, we give a representation lemma for the weak solution $u(x, t, \omega)$.

Lemma 5. ([31, Lemma 5]) *The weak solution u of equation (1) can be written as*

$$u(x, t, \omega) = I_t^\alpha g(t, \omega) f(x) + \int_0^t I_t^\alpha g(\tau, \omega) v_t(x, t - \tau) d\tau, \quad t \in (0, T], \quad (5)$$

where $v(x, t)$ is the solution of the following deterministic fractional diffusion equation

$$\begin{cases} \partial_t^\alpha v + \mathcal{A}v = 0, & (x, t) \in D \times (0, T], \\ v(x, t) = 0, & (x, t) \in \partial D \times (0, T], \\ v(x, 0) = f(x), & x \in D. \end{cases} \quad (6)$$

3 Main result

3.1 Moments representation

With Lemmas 1 and 5, the moments we used can be represented in terms of the unknowns g_1, g_2 . See the lemma below.

Lemma 6.

$$\begin{aligned} \mathbb{E}[I_t^{1-\alpha} u(x_0, t, \omega)] &= \int_0^t g_1(\tau) v(x_0, t - \tau) d\tau, \\ \mathbb{V}[I_t^{1-\alpha} u(x_0, t, \omega)] &= \int_0^t g_2^2(\tau) [v(x_0, t - \tau)]^2 d\tau, \quad t \in (0, T]. \end{aligned} \quad (7)$$

Proof. With Lemma 5 and the fact that

$$\int_s^t (t - \tau)^{-\alpha} (\tau - s)^{\alpha-1} d\tau = B(1 - \alpha, \alpha) = \Gamma(1 - \alpha) \Gamma(\alpha) / \Gamma(1),$$

here B is the Beta function, the next result can be deduced,

$$\begin{aligned} I_t^{1-\alpha} u(x, t, \omega) &= \frac{f(x)}{\Gamma(\alpha) \Gamma(1 - \alpha)} \int_0^t (t - \tau)^{-\alpha} \int_0^\tau (\tau - s)^{\alpha-1} g(s, \omega) ds d\tau \\ &\quad + \frac{1}{\Gamma(1 - \alpha)} \int_0^t (t - \tau)^{-\alpha} \int_0^\tau I_t^\alpha g(\tau - s, \omega) v_t(x, s) ds d\tau \\ &= \frac{1}{\Gamma(\alpha) \Gamma(1 - \alpha)} \left[f(x) \int_0^t g(s, \omega) \int_s^t (t - \tau)^{-\alpha} (\tau - s)^{\alpha-1} d\tau ds \right. \\ &\quad \left. + \int_0^t v_t(x, s) \int_0^{t-s} g(r, \omega) \int_{r+s}^t (t - \tau)^{-\alpha} (\tau - s - r)^{1-\alpha} d\tau dr ds \right] \\ &= f(x) \int_0^t g(s, \omega) ds + \int_0^t v_t(x, s) \int_0^{t-s} g(r, \omega) dr ds \end{aligned}$$

$$\begin{aligned}
&= f(x) \int_0^t g(s, \omega) ds + \int_0^t g(r, \omega) [v(x, t-r) - v(x, 0)] dr \\
&= \int_0^t g(\tau, \omega) v(x, t-\tau) d\tau.
\end{aligned}$$

Then we have

$$I_t^{1-\alpha} u(x_0, t, \omega) = \int_0^t g_1(\tau) v(x_0, t-\tau) d\tau + \int_0^t g_2(\tau) v(x_0, t-\tau) d\mathbb{W}(\tau).$$

Applying Ito formula in Lemma 1 to the above equality leads to (7). \square

Remark 1. In [31], the authors use integration by parts on the right side of (7) to deduce the following second kind Volterra equations,

$$\begin{aligned}
G_1(t) &= f^{-1}(x_0) \mathbb{E}[I_t^{1-\alpha} u(x_0, t, \omega)] - f^{-1}(x_0) \int_0^t G_1(\tau) v_t(x_0, t-\tau) d\tau, \\
G_2(t) &= f^{-2}(x_0) \mathbb{V}[I_t^{1-\alpha} u(x_0, t, \omega)] - 2f^{-2}(x_0) \int_0^t G_2(\tau) v(x_0, t-\tau) v_t(x_0, t-\tau) d\tau,
\end{aligned}$$

where

$$G_1(t) = \int_0^t g_1(\tau) d\tau, \quad G_2(t) = \int_0^t g_2^2(\tau) d\tau.$$

However, since $f(x_0) = 0$ in this work, we can only start the analysis from (7). Due to the convolution structure, the estimates of the unknowns on the partial interval $(0, T-\eta)$ are attained. See the next subsection for details.

3.2 Proof of Theorem 1

From (7), we build the proof of Theorem 1.

Proof of Theorem 1 (a). Let $T_1 = 0$, $T_2 + \eta = T$, then inserting (2) to (7) straightforwardly yields that

$$\|\mathbb{E}[I_t^{1-\alpha} u(x_0, t, \omega)]\|_{L^1(0, T)} \geq \|g_1\|_{L^1(0, T-\eta)} \|v(x_0, \cdot)\|_{L^1(0, \eta)}.$$

For the left side, we have

$$\begin{aligned}
\|\mathbb{E}[I_t^{1-\alpha} u(x_0, t, \omega)]\|_{L^1(0, T)} &\leq \frac{1}{\Gamma(1-\alpha)} \mathbb{E} \left[\int_0^T \int_0^t (t-\tau)^{-\alpha} |u(x_0, \tau, \omega)| d\tau dt \right] \\
&= \frac{1}{\Gamma(2-\alpha)} \mathbb{E} \left[\int_0^T (T-\tau)^{1-\alpha} |u(x_0, \tau, \omega)| d\tau \right] \\
&\leq C_\alpha T^{1-\alpha} \mathbb{E} [\|u(x_0, \cdot, \omega)\|_{L^1(0, T)}],
\end{aligned}$$

then

$$\|g_1\|_{L^1(0,T-\eta)} \leq C_\alpha B_\eta T^{1-\alpha} \mathbb{E}[\|u(x_0, \cdot, \omega)\|_{L^1(0,T)}].$$

□

Proof of Theorem 1 (b). Let $\eta > 0$ be small and assume that g_1 changes sign on $0 < t_1 < t_2 < \dots < t_N < T - \eta$, for convenience, we set $t_0 = 0$ and $t_{N+1} = T - \eta$. By (7), for $t \geq t_k$, we can write

$$\int_{t_k}^t g_1(\tau) v(x_0, t - \tau) d\tau = \mathbb{E}[I_t^{1-\alpha} u(x_0, t, \omega)] - \sum_{j=1}^k S_j,$$

where

$$S_j = \int_{t_{j-1}}^{t_j} g_1(\tau) v(x_0, t - \tau) d\tau.$$

Using (3) to the above equality with $T_1 = t_k$, $T_2 = t_{k+1}$, we can obtain that for $k = 0, \dots, N$,

$$\begin{aligned} \|g_1\|_{L^1(t_k, t_{k+1})} &\leq B_\eta \left\| \int_{t_k}^t g_1(\tau) v(x_0, t - \tau) d\tau \right\|_{L^1(t_k, t_{k+1} + \eta)} + 2\|g_1\|_{L^1(t_{k+1}, t_{k+1} + \eta)} \\ &\leq B_\eta \left(\left\| \mathbb{E}[I_t^{1-\alpha} u(x_0, t, \omega)] \right\|_{L^1(t_k, t_{k+1} + \eta)} + \sum_{j=1}^k \|S_j\|_{L^1(t_k, t_{k+1} + \eta)} \right) \\ &\quad + 2\|g_1\|_{L^1(t_{k+1}, t_{k+1} + \eta)}. \end{aligned} \quad (8)$$

For $\|g_1\|_{L^1(t_{k+1}, t_{k+1} + \eta)}$, from the condition that $\|g_1\|_{L^\infty(0,T)} \leq M$ we have

$$\|g_1\|_{L^1(t_{k+1}, t_{k+1} + \eta)} = \int_{t_{k+1}}^{t_{k+1} + \eta} |g_1(\tau)| d\tau \leq M\eta. \quad (9)$$

For $\|S_j\|_{L^1(t_k, t_{k+1} + \eta)}$, it holds that

$$\begin{aligned} \|S_j\|_{L^1(t_k, t_{k+1} + \eta)} &\leq \int_{t_k}^{t_{k+1} + \eta} \int_{t_{j-1}}^{t_j} |g_1(\tau)| v(x_0, t - \tau) d\tau dt \\ &= \int_{t_{j-1}}^{t_j} |g_1(\tau)| \int_{t_k}^{t_{k+1} + \eta} v(x_0, t - \tau) dt d\tau \\ &= \int_{t_{j-1}}^{t_j} |g_1(\tau)| \|v(x_0, \cdot)\|_{L^1(t_k - \tau, t_{k+1} + \eta - \tau)} d\tau. \end{aligned}$$

Assumption 1 and Lemma 3 give that $|v(x_0, t)| \leq C_f$. Consequently,

$$\|S_j\|_{L^1(t_k, t_{k+1} + \eta)} \leq C_f T \|g_1\|_{L^1(t_{j-1}, t_j)}, \quad j = 1, \dots, k. \quad (10)$$

Inserting (9) and (10) into (8) yields that

$$\|g_1\|_{L^1(t_k, t_{k+1})} \leq B_\eta \left\| \mathbb{E}[I_t^{1-\alpha} u(x_0, t, \omega)] \right\|_{L^1(t_k, t_{k+1}+\eta)} + B_\eta C_f T \|g_1\|_{L^1(0, t_k)} + 2M\eta. \quad (11)$$

Fix $k = 0$, we have

$$\|g_1\|_{L^1(0, t_1)} \leq B_\eta \left\| \mathbb{E}[I_t^{1-\alpha} u(x_0, t, \omega)] \right\|_{L^1(0, t_1+\eta)} + 2M\eta. \quad (12)$$

Now we claim that for $k = 1, \dots, N+1$,

$$\|g_1\|_{L^1(0, t_k)} \leq \frac{(B_\eta C_f T + 1)^k - 1}{B_\eta C_f T} \left(B_\eta \left\| \mathbb{E}[I_t^{1-\alpha} u(x_0, t, \omega)] \right\|_{L^1(0, t_k+\eta)} + 2M\eta \right),$$

and prove it by induction. The case of $k = 1$ is valid by (12). Now assume that the claim holds for $k = l$, then for $k = l + 1$, the estimate (11) gives that

$$\begin{aligned} \|g_1\|_{L^1(0, t_{l+1})} &\leq \|g_1\|_{L^1(0, t_l)} + B_\eta \left\| \mathbb{E}[I_t^{1-\alpha} u(x_0, t, \omega)] \right\|_{L^1(t_l, t_{l+1}+\eta)} + B_\eta C_f T \|g_1\|_{L^1(0, t_l)} + 2M\eta \\ &\leq (B_\eta C_f T + 1) \frac{(B_\eta C_f T + 1)^l - 1}{B_\eta C_f T} \left(B_\eta \left\| \mathbb{E}[I_t^{1-\alpha} u(x_0, t, \omega)] \right\|_{L^1(0, t_l+\eta)} + 2M\eta \right) \\ &\quad + B_\eta \left\| \mathbb{E}[I_t^{1-\alpha} u(x_0, t, \omega)] \right\|_{L^1(t_l, t_{l+1}+\eta)} + 2M\eta \\ &\leq \frac{(B_\eta C_f T + 1)^{l+1} - 1}{B_\eta C_f T} \left(B_\eta \left\| \mathbb{E}[I_t^{1-\alpha} u(x_0, t, \omega)] \right\|_{L^1(0, t_{l+1}+\eta)} + 2M\eta \right). \end{aligned}$$

So the claim is valid, and recalling that $t_{N+1} = T - \eta$, we have

$$\begin{aligned} \|g_1\|_{L^1(0, T-\eta)} &\leq \frac{(B_\eta C_f T + 1)^{N+1} - 1}{B_\eta C_f T} \left(B_\eta \left\| \mathbb{E}[I_t^{1-\alpha} u(x_0, t, \omega)] \right\|_{L^1(0, T)} + 2M\eta \right) \\ &\leq \frac{(B_\eta C_f T + 1)^{N+1} - 1}{B_\eta C_f T} (C_\alpha B_\eta T^{1-\alpha} \mathbb{E}[\|u(x_0, \cdot, \omega)\|_{L^1(0, T)}] + 2M\eta). \end{aligned}$$

The proof is complete. \square

Proof of Theorem 1 (c). Note that g_2^2 keeps its sign on $(0, T)$. Analogous to the proof of Theorem 1 (a), setting $T_1 = 0$, $T_2 = T - \eta$ in (2), then (7) gives that

$$\begin{aligned} \left\| \mathbb{V}[I_t^{1-\alpha} u(x_0, t, \omega)] \right\|_{L^1(0, T)} &\geq \|g_2^2\|_{L^1(0, T-\eta)} \|v(x_0, \cdot)\|_{L^1(0, \eta)}^2 \\ &= \|g_2\|_{L^2(0, T-\eta)}^2 \|v(x_0, \cdot)\|_{L^2(0, \eta)}^2. \end{aligned}$$

Holder inequality yields that

$$\|v(x_0, \cdot)\|_{L^2(0, \eta)} \geq \|1\|_{L^2(0, \eta)}^{-1} \|v(x_0, \cdot)\|_{L^1(0, \eta)} = \eta^{-1/2} B_\eta^{-1}.$$

Consequently,

$$\|g_2\|_{L^2(0,T-\eta)} \leq \eta^{1/2} B_\eta \left\| \mathbb{V}[I_t^{1-\alpha} u(x_0, t, \omega)] \right\|_{L^1(0,T)}^{1/2}.$$

The proof of Theorem 1 is complete. \square

4 Numerical reconstruction

4.1 Regularized Levenberg-Marquardt iteration

The discretized formulation of integral equation (7) is derived as follows. Denote the uniform mesh on the interval $[0, T]$ as $\{0 = t_0 < t_1 < \dots < t_N = T\}$ and set $\Delta_t = T/N$. From Lemmas 3 and 4, we have $\{t \in [0, T] : v(x_0, t) = 0\}$ is at most a finite set. Thus we can set

$$v(x_0, t_1) > 0, \quad (13)$$

if the mesh size Δ_t is chosen appropriately.

Define

$$E(t_n) = \mathbb{E}[I_t^{1-\alpha} u(x_0, t_n, \omega)], \quad V(t_n) = \mathbb{V}[I_t^{1-\alpha} u(x_0, t_n, \omega)].$$

Then from (7) we have

$$\begin{aligned} E(t_n) &= \int_0^{t_n} g_1(\tau) v(x_0, t_n - \tau) d\tau = \sum_{k=1}^n \int_{t_{k-1}}^{t_k} g_1(\tau) v(x_0, t_n - \tau) d\tau \\ &\approx \Delta_t \sum_{k=1}^n [g_1(t_{k-1}) v(x_0, t_n - t_{k-1}) + g_1(t_k) v(x_0, t_n - t_k)] / 2 \\ &= \Delta_t \left[g_1(0) v(x_0, t_n) / 2 + g_1(t_n) v(x_0, 0) / 2 + \sum_{k=1}^{n-1} g_1(t_k) v(x_0, t_{n-k}) \right] \\ &= \Delta_t \left[g_1(0) v(x_0, t_n) / 2 + \sum_{k=1}^{n-1} g_1(t_k) v(x_0, t_{n-k}) \right], \end{aligned}$$

where the last equality comes from $v(x_0, 0) = f(x_0) = 0$. Analogously,

$$V(t_n) = \Delta_t \left[g_2^2(0) v^2(x_0, t_n) / 2 + \sum_{k=1}^{n-1} g_2^2(t_k) v^2(x_0, t_{n-k}) \right].$$

From the above results, we can give the discretized formulation of (7),

$$A_1 \vec{g}_1 = \vec{E}, \quad A_2 \vec{g}_2 = \vec{V}, \quad (14)$$

where

$$\vec{g}_1 = \begin{bmatrix} g_1(t_0) \\ \vdots \\ g_1(t_{N-1}) \end{bmatrix}, \quad \vec{g}_2 = \begin{bmatrix} g_2^2(t_0) \\ \vdots \\ g_2^2(t_{N-1}) \end{bmatrix}, \quad \vec{E} = \begin{bmatrix} E(t_1) \\ \vdots \\ E(t_N) \end{bmatrix}, \quad \vec{V} = \begin{bmatrix} V(t_1) \\ \vdots \\ V(t_N) \end{bmatrix},$$

and the matrices A_1, A_2 are given as

$$A_1 = \Delta_t \begin{bmatrix} v(x_0, t_1)/2 & & & \\ v(x_0, t_2)/2 & v(x_0, t_1) & & \\ \vdots & \vdots & \ddots & \\ v(x_0, t_N)/2 & v(x_0, t_{N-1}) & \cdots & v(x_0, t_1) \end{bmatrix},$$

$$A_2 = \Delta_t \begin{bmatrix} v^2(x_0, t_1)/2 & & & \\ v^2(x_0, t_2)/2 & v^2(x_0, t_1) & & \\ \vdots & \vdots & \ddots & \\ v^2(x_0, t_N)/2 & v^2(x_0, t_{N-1}) & \cdots & v^2(x_0, t_1) \end{bmatrix}.$$

From the definitions of \vec{g}_1, \vec{g}_2 , we can only recover the unknowns on the partial interval $[0, t_{N-1}] = [0, T - \Delta_t]$, which indicates Theorem 1.

In practice, considering the measured error, the noisy moments $\vec{E}_\delta, \vec{V}_\delta$ will be used instead of \vec{E}, \vec{V} , and it holds that $\|(\vec{E}_\delta - \vec{E})/\vec{E}\|_\infty \leq \delta$, $\|(\vec{V}_\delta - \vec{V})/\vec{V}\|_\infty \leq \delta$. Due to the ill-posedness of this inverse problem, we choose the regularized Levenberg-Marquardt iteration [28, 36, 38] to solve the noisy equation (14), in which $\vec{E}_\delta, \vec{V}_\delta$ are used. The iteration is given as follows,

$$\begin{aligned} \vec{g}_{1,k+1} &= \vec{g}_{1,k} + (A_1^T A_1 + \gamma_1 I)^{-1} A_1^T (\vec{E}_\delta - A_1 \vec{g}_{1,k}) \\ &= B_{1,\gamma_1} \vec{g}_{1,k} + (A_1^T A_1 + \gamma_1 I)^{-1} A_1^T \vec{E}_\delta, \\ \vec{g}_{2,k+1} &= \vec{g}_{2,k} + (A_2^T A_2 + \gamma_2 I)^{-1} A_2^T (\vec{V}_\delta - A_2 \vec{g}_{2,k}) \\ &= B_{2,\gamma_2} \vec{g}_{2,k} + (A_2^T A_2 + \gamma_2 I)^{-1} A_2^T \vec{V}_\delta, \end{aligned} \tag{15}$$

where

$$B_{l,\gamma_l} = I - (A_l^T A_l + \gamma_l I)^{-1} A_l^T A_l, \quad l = 1, 2,$$

and the regularization parameters γ_1, γ_2 are chosen as small positive constants.

4.2 Convergence of iteration (15)

The spectral radius of a square matrix, which is denoted by $\rho(\cdot)$, is defined as the largest absolute value of its eigenvalues. The next lemma concerns the spectral radius of the matrices B_{l,γ_l} , $l = 1, 2$, and after that the convergence of (15) is proved.

Lemma 7. $\rho(B_{l,\gamma_l}) < 1$, $l = 1, 2$.

Proof. Let (λ, \vec{y}) be one eigenpair of B_{1,γ_1} with $\vec{y} \neq \vec{0}$. We need to show that $|\lambda| < 1$. From $B_{1,\gamma_1}\vec{y} = \lambda\vec{y}$, we can deduce that

$$\lambda(A_1^T A_1 + \gamma_1 I)\vec{y} = \gamma_1 \vec{y}.$$

Taking inner product with \vec{y} yields that

$$\gamma_1 \langle \vec{y}, \vec{y} \rangle = \lambda \langle (A_1^T A_1 + \gamma_1 I)\vec{y}, \vec{y} \rangle = \lambda (\langle A_1 \vec{y}, A_1 \vec{y} \rangle + \gamma_1 \langle \vec{y}, \vec{y} \rangle),$$

which gives

$$|\lambda| = \left| \frac{\gamma_1 \|\vec{y}\|_2^2}{\|A_1 \vec{y}\|_2^2 + \gamma_1 \|\vec{y}\|_2^2} \right|.$$

Condition (13) ensures the invertibility of A_1 , which together with $\vec{y} \neq \vec{0}$ gives $\|A_1 \vec{y}\|_2^2 > 0$. Hence, considering that γ_1 is chosen as a small positive constant, we have

$$0 < \gamma_1 \|\vec{y}\|_2^2 < \|A_1 \vec{y}\|_2^2 + \gamma_1 \|\vec{y}\|_2^2,$$

which yields $|\lambda| < 1$.

The case for B_{2,γ_2} can be proved analogously. The proof is complete. \square

Proposition 2. *The sequences $\{\vec{g}_{1,k}\}_{k=0}^\infty, \{\vec{g}_{2,k}\}_{k=0}^\infty$ generated from iteration (15) are both convergent. Also, if we denote the limits by $\vec{g}_{1,\delta}$ and $\vec{g}_{2,\delta}$, respectively, then*

$$\lim_{\delta \rightarrow 0+} \|\vec{g}_{1,\delta} - \vec{g}_1\|_\infty = \lim_{\delta \rightarrow 0+} \|\vec{g}_{2,\delta} - \vec{g}_2\|_\infty = 0,$$

where \vec{g}_1, \vec{g}_2 solve equation (14).

Proof. The convergence follows from Lemma 7 straightforwardly.

From (15), we have

$$\vec{g}_{1,\delta} = (A_1^T A_1)^{-1} A_1^T \vec{E}_\delta, \quad \vec{g}_{2,\delta} = (A_2^T A_2)^{-1} A_2^T \vec{V}_\delta.$$

Considering the results $\vec{g}_1 = (A_1^T A_1)^{-1} A_1^T \vec{E}$, $\vec{g}_2 = (A_2^T A_2)^{-1} A_2^T \vec{V}$ and

$$\lim_{\delta \rightarrow 0+} \|\vec{E} - \vec{E}_\delta\|_\infty = \lim_{\delta \rightarrow 0+} \|\vec{V} - \vec{V}_\delta\|_\infty = 0,$$

it follows that $\vec{g}_{l,\delta} \rightarrow \vec{g}_l$, $l = 1, 2$ in the sense of $\|\cdot\|_\infty$ as $\delta \rightarrow 0+$. \square

4.3 Forward problem solver

To obtain the measurements, the direct problem of equation (1) should be considered. We first introduce the finite element method, and then the GMsFEM[13] to handle the case that κ is highly heterogeneous.

On space x , the piecewise linear basis $\{\phi_j(x)\}_{j=1}^m$ is used with $\phi_j = 0$ on ∂D and $\phi_j(x_k) = \delta_{jk}$, where $\{x_j\}_{j=1}^m$ consist of a Delaunay triangulation \mathcal{T}^h on domain D , and $h > 0$ is the fine mesh size. Then we define the finite element space as $\mathcal{V}_m = \text{span}\{\phi_j(x) : j = 1, \dots, m\}$. With this space, the projection operator $P_m : L^2(D) \mapsto \mathcal{V}_m$ can be given as

$$P_m \psi(x) = \sum_{j=1}^m \psi(x_j) \phi_j(x) =: \tilde{\psi}(x).$$

Here we use the notation $\tilde{\psi}$ for short and the corresponding vector form is denoted by $\vec{\psi} = [\psi(x_j)]_{j=1}^m$.

Writing

$$\tilde{u}(x, t, \omega) = \sum_{j=1}^m u(x_j, t, \omega) \phi_j(x), \quad \tilde{f}(x) = \sum_{j=1}^m f(x_j) \phi_j(x),$$

then the weak formulation of equation (1) with test function ϕ_i is

$$\sum_{j=1}^m \partial_t^\alpha u(x_j, t, \omega) \langle \phi_j, \phi_i \rangle_{L^2(D)} + \sum_{j=1}^m u(x_j, t, \omega) \langle \mathcal{A} \phi_j, \phi_i \rangle_{L^2(D)} = g(t, \omega) \sum_{j=1}^m f(x_j) \langle \phi_j, \phi_i \rangle_{L^2(D)}.$$

From the above formulation, we define the mass matrix \vec{M} and stiff matrix \vec{S} w.r.t. basis $\{\phi_j\}_{j=1}^m$ as

$$\vec{M} = \left[\langle \phi_j, \phi_i \rangle_{L^2(D)} \right]_{i,j=1}^m, \quad \vec{S} = \left[\langle \mathcal{A} \phi_j, \phi_i \rangle_{L^2(D)} \right]_{i,j=1}^m,$$

which will be used to construct the discretized scheme for equation (1).

For the discretization on time, the L_1 -stepping scheme [23, 44] is used. Again we use the uniform time mesh $0 = t_0 < t_1 < \dots < t_N = T$ and denote $\Delta_t = T/N$. Then the fractional derivative ∂_t^α is approximated as

$$\begin{aligned} \partial_t^\alpha \psi(t_1) &\approx b_{1,0}(\psi(t_1) - \psi(t_0)), \\ \partial_t^\alpha \psi(t_n) &\approx \sum_{k=1}^{n-1} (b_{n,k-1} - b_{n,k}) \psi(t_k) + b_{n,n-1} \psi(t_n) - b_{n,0} \psi(t_0), \quad n = 2, \dots, N, \end{aligned}$$

with parameters

$$b_{n,k} = \Gamma(2 - \alpha)^{-1} \Delta_t^{-\alpha} [(n - k)^{1-\alpha} - (n - k - 1)^{1-\alpha}], \quad k = 0, \dots, n - 1.$$

For the random term $g(t_n, \omega) = g_1(t_n) + g_2(t_n) \dot{\mathbb{W}}(t_n)$, due to $\mathbb{W}(t) - \mathbb{W}(s) \sim \mathcal{N}(0, t - s)$, we have

$$\dot{\mathbb{W}}(t_n) \approx [\mathbb{W}(t_n) - \mathbb{W}(t_{n-1})] / \Delta_t \sim \Delta_t^{-1/2} \mathcal{N}(0, 1).$$

Hence, considering the vanishing initial condition, the finite element scheme for solving equation (1) is given as: for $n = 1, \dots, N$, find the vector form \vec{u}_n of $\tilde{u}(x, t_n, \omega) \in \mathcal{V}_m$ such that

$$\begin{aligned} (b_{1,0}\vec{M} + \vec{S}) \vec{u}_1 &= \vec{M} \left(g_1(t_1)\vec{f} + g_2(t_1)\Delta_t^{-1/2}\mathcal{N}(0,1)\vec{f} \right), \\ (b_{n,n-1}\vec{M} + \vec{S}) \vec{u}_n &= \vec{M} \left(g_1(t_n)\vec{f} + g_2(t_n)\Delta_t^{-1/2}\mathcal{N}(0,1)\vec{f} \right) + \sum_{k=1}^{n-1} (b_{n,k} - b_{n,k-1})\vec{u}_k. \end{aligned} \quad (16)$$

Following this scheme, the solution $v(x, t)$ of equation (6) can be simulated similarly.

4.3.1 GMsFEM

In many practical applications, the coefficient $\kappa(x)$ can be highly heterogeneous, in which very fine mesh is required in the finite element method, accompanied with huge computational cost. So we choose the Generalized Multiscale Finite Element Method (GMsFEM [13]) as the model reduction technique here. The GMsFEM provides a systematic way of reducing the computational cost in solving various types of highly heterogeneous partial differential equations [15, 16, 48, 11]. This method reduces the degrees of freedom of large systems by constructing appropriate multiscale basis functions, which are only needed to calculate one time. Therefore GMsFEM is particular suitable for the computing that requires solving a fixed equation repetitively but with different source or boundary conditions. Besides, by choosing different number of basis, we can easily tune the accuracy of the solution, which may be useful in inverse problems based on the recent research [46].

In GMsFEM, there are two stages to construct the generalized multiscale basis: the snapshot stage and offline stage. We consider a triangulation of domain D denoted

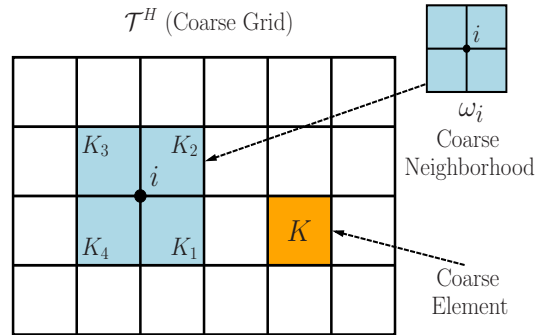


Figure 1: Illustration of coarse neighborhood and coarse element.

by \mathcal{T}^H such that \mathcal{T}^h is its refinement. Let \mathcal{S}^H be the set of all coarse grid nodes and $N_S = |\mathcal{S}^H|$. Elements of \mathcal{T}^H are called coarse grid blocks. For each vertex $x_i \in \mathcal{S}^H$

in the grid \mathcal{T}^H , we define the coarse neighborhood ω_i by

$$\omega_i = \bigcup \{K_j : K_j \subset \mathcal{T}^H, x_i \in K_j\}.$$

That is, ω_i is the union of all coarse grid blocks K_j containing the vertex x_i , see Figure 1. We will construct multiscale basis functions in each coarse neighborhood ω_i .

We begin by the construction of local snapshot spaces in ω_i . There are two types of local snapshot spaces. The first type is

$$\mathcal{V}_1^{i,\text{snap}} = \mathcal{V}_m(\omega_i),$$

where $\mathcal{V}_m(\omega_i)$ is the restriction of the \mathcal{V}_m to ω_i . Therefore, $\mathcal{V}_1^{i,\text{snap}}$ contains all possible fine scale functions defined on ω_i . The second type is the harmonic extension space. More specifically, let $\mathcal{V}_m(\partial\omega_i)$ be the restriction of the conforming space to $\partial\omega_i$. Then we define the fine-grid delta function $\delta_k \in \mathcal{V}_m(\partial\omega_i)$ on $\partial\omega_i$ by

$$\delta_k(x_l) = \begin{cases} 1, & l = k, \\ 0, & l \neq k, \end{cases}$$

where $\{x_l\}$ are all fine grid nodes on $\partial\omega_i$. Given δ_k , we seek u_k by

$$\begin{aligned} -\mathcal{A}u_k &= 0, & \text{in } \omega_i, \\ u_k &= \delta_k, & \text{on } \partial\omega_i. \end{aligned} \tag{17}$$

The linear span of the above harmonic extensions is our second type local snapshot space $\mathcal{V}_2^{i,\text{snap}}$. To simplify the presentations, we will use $\mathcal{V}^{i,\text{snap}}$ to denote $\mathcal{V}_1^{i,\text{snap}}$ or $\mathcal{V}_2^{i,\text{snap}}$ when there is no need to distinguish them. Moreover, we write

$$\mathcal{V}^{i,\text{snap}} = \text{span}\{\psi_k^{i,\text{snap}} : k = 1, 2, \dots, M^{i,\text{snap}}\},$$

where $\psi_k^{i,\text{snap}}$ is the snapshot functions, and $M^{i,\text{snap}}$ is the number of basis functions in $\mathcal{V}^{i,\text{snap}}$.

The dimension of the snapshot space is still too large for computation. We can use a spectral problem to select the dominant modes from the snapshot space. Specifically, in each neighborhood, we consider

$$\mathcal{A}\phi = \lambda\tilde{\kappa}\phi, \tag{18}$$

where $\tilde{\kappa} = \kappa \sum_{i=1}^{N_S} |\nabla \chi_i|^2$, N_S is the total number of neighborhoods, and χ_i is the partition of unity function [2] for ω_i . One choice of a partition of unity function is the coarse grid hat function whose value at the coarse vertex x_i is 1 and 0 at all other coarse vertices. Another choice of the basis function is introduced in [20]. We solve the above spectral problem (18) in the local snapshot space $\mathcal{V}^{i,\text{snap}}$. Then we use the first L_i eigenfunctions ϕ_i corresponding to the first L_i eigenvalues to construct the

local offline space. We define

$$\psi_l^{i,\text{off}} = \sum_{k=1}^{M^{i,\text{snap}}} \phi_{l,k} \psi_k^{i,\text{snap}}, \quad l = 1, 2, \dots, L_i,$$

where $\phi_{l,k}$ is the k -th component of ϕ_l . Note that the function $\psi_l^{i,\text{off}}$ is not globally continuous, therefore we need to multiply it with the partition of unity function. We define the local offline space as

$$\mathcal{V}_H^{i,\text{off}} = \text{span}\{\chi_i \psi_l^{i,\text{off}} : l = 1, 2, \dots, L_i\}.$$

Then, the offline space can be defined as

$$\mathcal{V}_H^{\text{off}} = \text{span}\{\mathcal{V}_H^{i,\text{off}} : i = 1, 2, \dots, N_S\}.$$

We note that equations (17), (18) are solved on the fine grid \mathcal{T}^h numerically. Then we can treat each discrete offline basis in \mathcal{V}^{off} as a column vector $\vec{\Phi}_i$, and denote $\vec{R} = [\vec{\Phi}_1, \dots, \vec{\Phi}_L]$ be the matrix that represents all the multiscale basis functions (total number $L = \sum_i N_S L_i$). Thus, the discretized scheme for solving equation (1) with GMsFEM is given as: for $\tilde{u}_{H,n} \in \mathcal{V}_H^{\text{off}}$, $n = 1, \dots, N$, its vector form $\vec{u}_{H,n}$ satisfies

$$\begin{aligned} (b_{1,0} \vec{M}_H + \vec{S}_H) \vec{u}_{H,1} &= \vec{M}_H \left(g_1(t_1) \vec{f}_H + g_2(t_1) \Delta_t^{-1/2} \mathcal{N}(0, 1) \vec{f}_H \right), \\ (b_{n,n-1} \vec{M}_H + \vec{S}_H) \vec{u}_{H,n} &= \vec{M}_H \left(g_1(t_n) \vec{f}_H + g_2(t_n) \Delta_t^{-1/2} \mathcal{N}(0, 1) \vec{f}_H \right. \\ &\quad \left. + \sum_{k=1}^{n-1} (b_{n,k} - b_{n,k-1}) \vec{u}_{H,k} \right), \end{aligned} \quad (19)$$

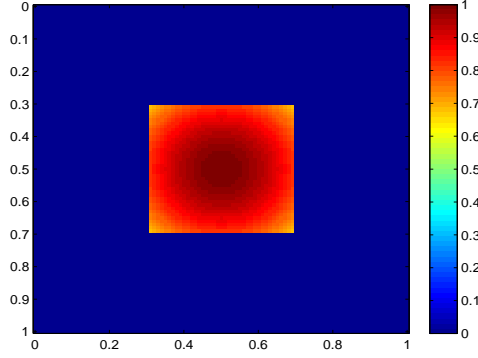
where $\vec{M}_H = \vec{R}^T \vec{M} \vec{R}$, $\vec{S}_H = \vec{R}^T \vec{S} \vec{R}$, $\vec{f}_H = \vec{R}^T \vec{f}$. Typically, we only need to select a few numbers of basis in a neighborhood, which ensures that the degrees of freedom of scheme (19) is much smaller comparing with scheme (16). After we obtain $\vec{u}_{H,n}$, one projects the solution into the space \mathcal{V}_m through $\vec{u}_{H,n}^h = \vec{R} \vec{u}_{H,n}$.

4.4 Numerical experiments

Now we present several numerical experiments to show the performance of our algorithm. We first consider the smooth case,

$$g_1(t) = t + \sin(2\pi t) + \sin(3\pi t), \quad g_2(t) = 0.5t + \sin(\pi t) - \sin(2\pi t).$$

We set $T = 1$, the spatial component $f(x)$ in source term is shown in Figure 2, and the observation point is chosen as $x_0 = (0.4, 0.2)$, which is out of $\text{supp}(f)$. In addition, 3×10^4 realizations of the single point data $u(x_0, t, \omega)$ are recorded, and 1% relative noise is added on the moments, i.e. $\delta = 1\%$.

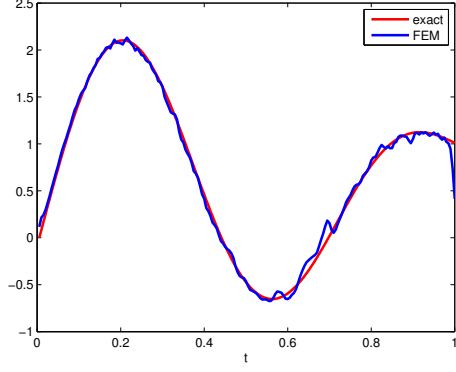


(a) $f(x)$

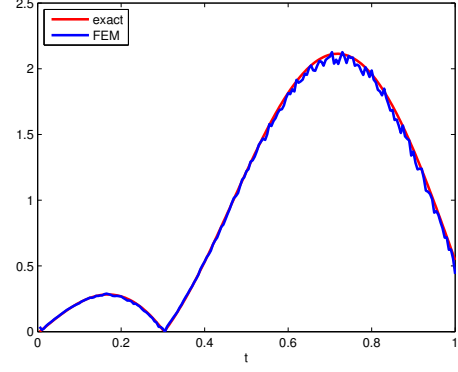
Figure 2: Spatial component $f(x)$.

We consider both the homogeneous and highly heterogeneous media cases. For the homogeneous case (test model 1), the model size is 50×50 . We apply FEM (16) for the forward modeling. The corresponding inversion results are presented in Figure 3. We can see our inversion algorithm (15) can generate satisfactory approximations of the targeted unknowns.

Two heterogeneous experiments are considered and the corresponding $\kappa(x)$ are shown in Figure 4. The size of these models is 100×100 , and in GMsFEM (19), we use a 10×10 coarse grid. Therefore, the degrees of freedom for the FEM system is 9801 and it is 242 for the GMsFEM with 2 bases, we can see huge reduction of the unknowns in forward modeling. The inversion results for the heterogeneous case are displayed in Figures 5 and 6. The comparisons of the approximations for g_1 and $|g_2|$ from the fine-grid FEM, the GMsFEM with two bases and the GMsFEM with one basis are displayed. It can be seen clearly that the GMsFEM with only one basis yields unjustifiable inversion results especially for test model 2. However, the results from GMsFEM with two bases is can be comparable with the FEM results and it is better than FEM for the approximation of $|g_2|$. This is not surprising according to [46], which tells us that more accurate forward modeling will not always yield better inversion performance. Also we note that the running time of FEM is about 15 times of GMsFEM, and more computational time saving is expected if the size of the model is larger. In addition, GMsFEM with one basis is actually the MsFEM basis [20], which is more suitable for highly oscillating media, it is an ideal choice to use spectral basis space for high-contrast media inversion.

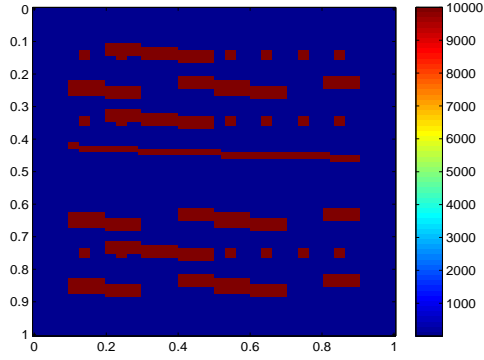


(a) Approximation comparison for g_1

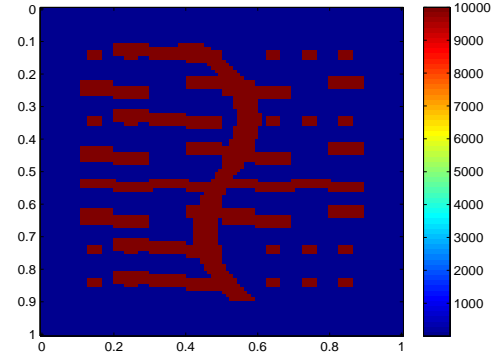


(b) Approximation comparison for $|g_2|$

Figure 3: Results for homogeneous model (test model 1), smooth case.

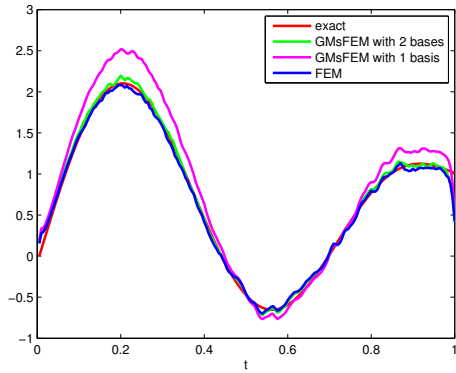


(a) test model 2

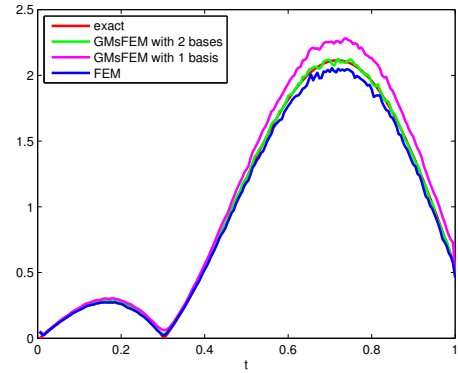


(b) test model 3

Figure 4: Heterogeneous test models.

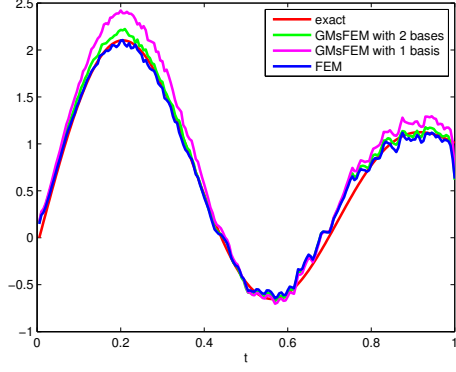


(a) Approximation comparison for g_1

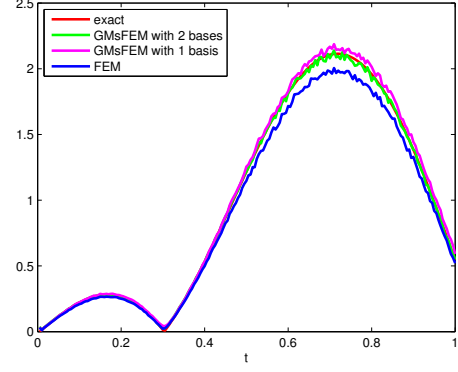


(b) Approximation comparison for $|g_2|$

Figure 5: Results for test model 2, smooth case.

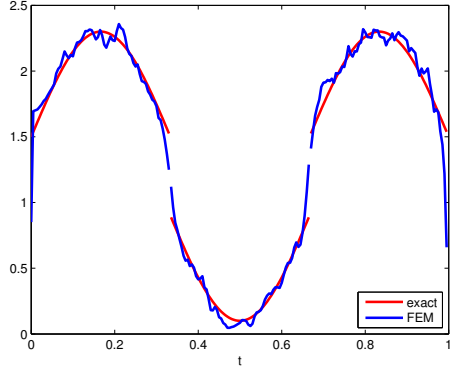


(a) Approximation comparison for g_1

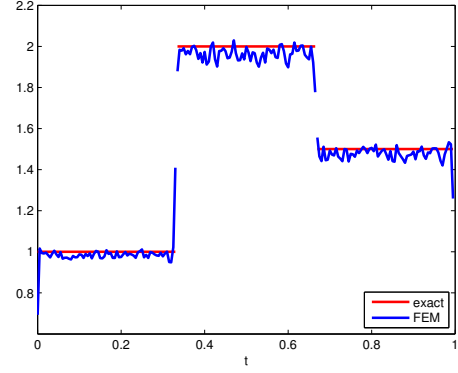


(b) Approximation comparison for $|g_2|$

Figure 6: Results for test model 3, smooth case.

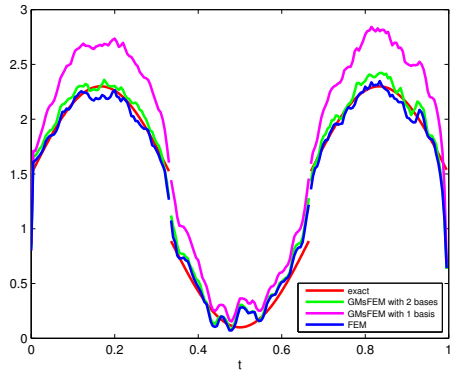


(a) Approximation comparison for g_1

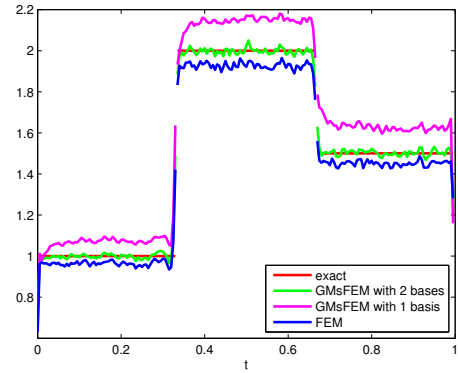


(b) Approximation comparison for $|g_2|$

Figure 7: Results for homogeneous model (test model 1), non-smooth case.



(a) Approximation comparison for g_1



(b) Approximation comparison for $|g_2|$

Figure 8: Results for test model 2, non-smooth case.

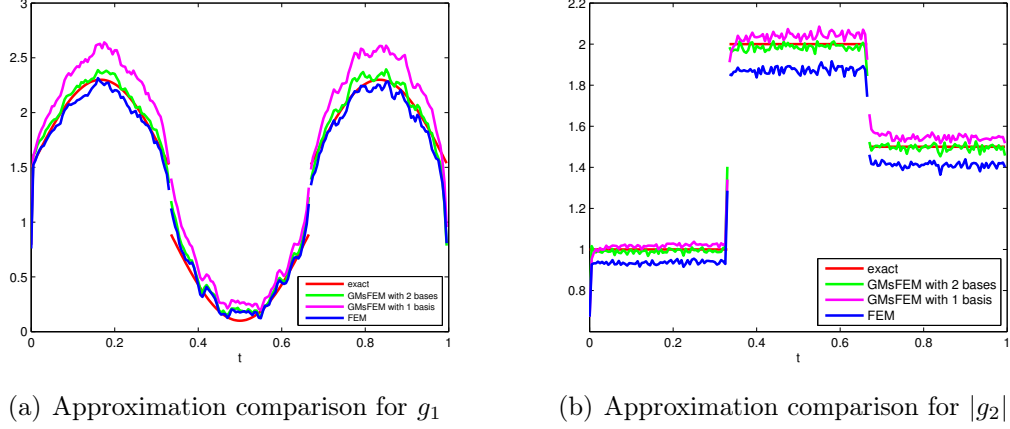


Figure 9: Results for test model 3, non-smooth case.

Furthermore, the non-smooth case is also tested,

$$\begin{aligned}
 g_1(t) &= (1.5 + 0.8 \sin(3\pi t)) \chi_{t \in [0, 1/3) \cup [2/3, 1]} + (0.9 + 0.8 \sin(3\pi t)) \chi_{t \in [1/3, 2/3)}, \\
 g_2(t) &= \chi_{t \in [0, 1/3)} - 2\chi_{t \in [1/3, 2/3)} + 1.5\chi_{t \in [2/3, 1]}.
 \end{aligned}$$

We present the corresponding results in Figures 7-9. Again, we observe that our algorithm works well, and the GMsFEM with 2 bases is better than the FEM especially for the approximation of $|g_2|$, which agrees with the smooth case.

5 Concluding remark and future work

This paper considers the recovery of unknown source in the stochastic fractional diffusion equation. The statistical moments of single point data $u(x_0, t, \omega)$ are used, and the observation point x_0 is set to be out of the support of the source, which fits the practical circumstance. The restriction on x_0 makes the analysis more challenging. Nonetheless, the estimates of unknowns on the incomplete interval are given, and the constructed iterative algorithm works for both smooth and non-smooth cases.

From the numerical results, one natural question for this inverse problem will be whether we can recover more information about the unknown $g_2(t)$. In this work, we can only solve g_2^2 , or $|g_2|$, which can not describe g_2 well. This comes from the Ito formula in Lemma 1, by which the term g_2^2 is generated. Hence, if we want to reconstruct g_2 further, some more complicated statistical moments need to be used, not only variance. For example, it seems that we may obtain $\pm g_2$ from the moment covariance. The corresponding investigation is one of our future work.

Acknowledgment

The second author was supported by Academy of Finland, grants 284715, 312110, and the Atmospheric mathematics project of University of Helsinki.

References

- [1] E. E. Adams and L. W. Gelhar. Field study of dispersion in a heterogeneous aquifer: 2. spatial moments analysis. *Water Resources Research*, 28(12):3293–3307, 1992.
- [2] I. Babuška and J. M. Melenk. The partition of unity method. *International journal for numerical methods in engineering*, 40(4):727–758, 1997.
- [3] G. Bao, C. Chen, and P. Li. Inverse random source scattering for elastic waves. *SIAM J. Numer. Anal.*, 55(6):2616–2643, 2017. URL: <https://doi.org/10.1137/16M1088922>, doi:10.1137/16M1088922.
- [4] G. Bao, T. Yin, and F. Zeng. Multifrequency iterative methods for the inverse medium scattering problems in elasticity. *SIAM J. Sci. Comput.*, 41(4):B721–B745, 2019. URL: <https://doi.org/10.1137/18M1220844>, doi:10.1137/18M1220844.
- [5] E. Barkai, R. Metzler, and J. Klafter. From continuous time random walks to the fractional fokker-planck equation. *Phys. Rev. E*, 61:132–138, Jan 2000. URL: <https://link.aps.org/doi/10.1103/PhysRevE.61.132>, doi:10.1103/PhysRevE.61.132.
- [6] B. Berkowitz, A. Cortis, M. Dentz, and H. Scher. Modeling non-fickian transport in geological formations as a continuous time random walk. *Reviews of Geophysics*, 44(2), 2006.
- [7] D. Bȃȃleanu and A. M. Lopes. *Handbook of Fractional Calculus with Applications*. De Gruyter, 2019.
- [8] J.-P. Bouchaud and A. Georges. Anomalous diffusion in disordered media: Statistical mechanisms, models and physical applications. *Physics Reports*, 195(4):127 – 293, 1990. URL: <http://www.sciencedirect.com/science/article/pii/037015739090099N>, doi:[https://doi.org/10.1016/0370-1573\(90\)90099-N](https://doi.org/10.1016/0370-1573(90)90099-N).
- [9] H. Y. Chan, E. Chung, and Y. Efendiev. Adaptive mixed gmsfem for flows in heterogeneous media. *Numerical Mathematics: Theory, Methods and Applications*, 9(4):497–527, 2016.
- [10] Y. Cho, R. L. Gibson, and S. Fu. Frequency-domain reverse time migration using generalized multiscale forward modeling. In *SEG Technical Program Expanded Abstracts 2017*, pages 4583–4588. Society of Exploration Geophysicists, 2017.

- [11] E. T. Chung, Y. Efendiev, and C. S. Lee. Mixed generalized multiscale finite element methods and applications. *Multiscale Modeling & Simulation*, 13(1):338–366, 2015.
- [12] E. T. Chung, Y. Efendiev, and G. Li. An adaptive gmsfem for high-contrast flow problems. *Journal of Computational Physics*, 273:54–76, 2014.
- [13] Y. Efendiev, J. Galvis, and T. Y. Hou. Generalized multiscale finite element methods (gmsfem). *Journal of Computational Physics*, 251:116–135, 2013.
- [14] X. Feng, P. Li, and X. Wang. An inverse random source problem for the time fractional diffusion equation driven by a fractional brownian motion. *arXiv preprint arXiv:1908.03666*, 2019.
- [15] S. Fu and K. Gao. A fast solver for the helmholtz equation based on the generalized multiscale finite-element method. *Geophysical Journal International*, 211(2):819–835, 2017.
- [16] J. Galvis, G. Li, and K. Shi. A generalized multiscale finite element method for the brinkman equation. *Journal of Computational and Applied Mathematics*, 280:294–309, 2015.
- [17] Y. Gefen, A. Aharony, and S. Alexander. Anomalous diffusion on percolating clusters. *Phys. Rev. Lett.*, 50:77–80, Jan 1983. URL: <https://link.aps.org/doi/10.1103/PhysRevLett.50.77>, doi:10.1103/PhysRevLett.50.77.
- [18] T. Ghosh, A. Rüland, M. Salo, and G. Uhlmann. Uniqueness and reconstruction for the fractional calderón problem with a single measurement. *Journal of Functional Analysis*, page 108505, 2020.
- [19] Y. Hatano and N. Hatano. Dispersive transport of ions in column experiments: An explanation of long-tailed profiles. *Water resources research*, 34(5):1027–1033, 1998.
- [20] T. Y. Hou and X.-H. Wu. A multiscale finite element method for elliptic problems in composite materials and porous media. *Journal of computational physics*, 134(1):169–189, 1997.
- [21] X. Huang, Z. Li, and M. Yamamoto. Carleman estimates for the time-fractional advection-diffusion equations and applications. *Inverse Problems*, 35(4):045003, 36, 2019. URL: <https://doi.org/10.1088/1361-6420/ab0138>, doi:10.1088/1361-6420/ab0138.
- [22] D. Jiang, Z. Li, Y. Liu, and M. Yamamoto. Weak unique continuation property and a related inverse source problem for time-fractional diffusion-advection equations. *Inverse Problems*, 33(5):055013, 22, 2017. URL: <https://doi.org/10.1088/1361-6420/aa58d1>, doi:10.1088/1361-6420/aa58d1.
- [23] B. Jin, R. Lazarov, and Z. Zhou. An analysis of the L1 scheme for the sub-diffusion equation with nonsmooth data. *IMA J. Numer. Anal.*, 36(1):197–

- 221, 2016. URL: <https://doi.org/10.1093/imanum/dru063>, doi:10.1093/imanum/dru063.
- [24] B. Jin and W. Rundell. A tutorial on inverse problems for anomalous diffusion processes. *Inverse Problems*, 31(3):035003, 40, 2015. URL: <https://doi.org/10.1088/0266-5611/31/3/035003>, doi:10.1088/0266-5611/31/3/035003.
- [25] A. A. Kilbas, H. M. Srivastava, and J. J. Trujillo. *Theory and applications of fractional differential equations*, volume 204 of *North-Holland Mathematics Studies*. Elsevier Science B.V., Amsterdam, 2006.
- [26] J. Klafter and R. Silbey. Derivation of the continuous-time random-walk equation. *Phys. Rev. Lett.*, 44:55–58, Jan 1980. URL: <https://link.aps.org/doi/10.1103/PhysRevLett.44.55>, doi:10.1103/PhysRevLett.44.55.
- [27] R.-Y. Lai, Y.-H. Lin, and A. R  land. The calder  on problem for a space-time fractional parabolic equation. *arXiv preprint arXiv:1905.08719*, 2019.
- [28] K. Levenberg. A method for the solution of certain non-linear problems in least squares. *Quarterly of applied mathematics*, 2(2):164–168, 1944.
- [29] Z. Li, Y. Kian, and E. Soccorsi. Initial-boundary value problem for distributed order time-fractional diffusion equations. *Asymptot. Anal.*, 115(1-2):95–126, 2019. URL: <https://doi.org/10.3233/asy-191532>, doi:10.3233/asy-191532.
- [30] Z. Li, Y. Liu, and M. Yamamoto. Initial-boundary value problems for multi-term time-fractional diffusion equations with positive constant coefficients. *Appl. Math. Comput.*, 257:381–397, 2015. URL: <https://doi.org/10.1016/j.amc.2014.11.073>, doi:10.1016/j.amc.2014.11.073.
- [31] C. Liu, J. Wen, and Z. Zhang. Reconstruction of the time-dependent source term in a stochastic fractional diffusion equation. *arXiv preprint arXiv:1911.00304*, 2019.
- [32] Y. Liu, W. Rundell, and M. Yamamoto. Strong maximum principle for fractional diffusion equations and an application to an inverse source problem. *Fract. Calc. Appl. Anal.*, 19(4):888–906, 2016. URL: <https://doi.org/10.1515/fca-2016-0048>, doi:10.1515/fca-2016-0048.
- [33] Y. Liu and Z. Zhang. Reconstruction of the temporal component in the source term of a (time-fractional) diffusion equation. *J. Phys. A*, 50(30):305203, 27, 2017. URL: <https://doi.org/10.1088/1751-8121/aa763a>, doi:10.1088/1751-8121/aa763a.
- [34] Y. Luchko. Maximum principle for the generalized time-fractional diffusion equation. *J. Math. Anal. Appl.*, 351(1):218–223, 2009. URL: <https://doi.org/10.1016/j.jmaa.2008.10.018>, doi:10.1016/j.jmaa.2008.10.018.
- [35] F. Mainardi. *Fractional calculus and waves in linear viscoelasticity*. Imperial College Press, London, 2010. An introduction to mathematical models. URL: <http://dx.doi.org/10.1142/9781848163300>, doi:10.1142/9781848163300.

- [36] D. W. Marquardt. An algorithm for least-squares estimation of nonlinear parameters. *J. Soc. Indust. Appl. Math.*, 11:431–441, 1963.
- [37] R. Metzler, J.-H. Jeon, A. G. Cherstvy, and E. Barkai. Anomalous diffusion models and their properties: non-stationarity, non-ergodicity, and ageing at the centenary of single particle tracking. *Physical Chemistry Chemical Physics*, 16(44):24128–24164, 2014.
- [38] J. J. Moré. The Levenberg-Marquardt algorithm: implementation and theory. In *Numerical analysis (Proc. 7th Biennial Conf., Univ. Dundee, Dundee, 1977)*, pages 105–116. Lecture Notes in Math., Vol. 630, 1978.
- [39] R. Nigmatullin. The realization of the generalized transfer equation in a medium with fractal geometry. *physica status solidi (b)*, 133(1):425–430, 1986.
- [40] P. Niu, T. Helin, and Z. Zhang. An inverse random source problem in a stochastic fractional diffusion equation. *Inverse Problems*, 2019.
- [41] B. Øksendal. *Stochastic differential equations*. Universitext. Springer-Verlag, Berlin, sixth edition, 2003. An introduction with applications. URL: <https://doi.org/10.1007/978-3-642-14394-6>.
- [42] A. Rüland and M. Salo. The fractional Calderón problem: Low regularity and stability. *Nonlinear Anal.*, 193:111529, 2020. URL: <https://doi.org/10.1016/j.na.2019.05.010>, doi:10.1016/j.na.2019.05.010.
- [43] W. Rundell and Z. Zhang. Fractional diffusion: recovering the distributed fractional derivative from overposed data. *Inverse Problems*, 33(3):035008, 27, 2017. URL: <https://doi.org/10.1088/1361-6420/aa573e>, doi:10.1088/1361-6420/aa573e.
- [44] W. Rundell and Z. Zhang. Recovering an unknown source in a fractional diffusion problem. *J. Comput. Phys.*, 368:299–314, 2018. URL: <https://doi.org/10.1016/j.jcp.2018.04.046>, doi:10.1016/j.jcp.2018.04.046.
- [45] S. G. Samko, A. A. Kilbas, and O. I. Marichev. *Fractional integrals and derivatives*. Gordon and Breach Science Publishers, Yverdon, 1993. Theory and applications, Edited and with a foreword by S. M. Nikol’skiĭ, Translated from the 1987 Russian original, Revised by the authors.
- [46] D. Smyl and D. Liu. Less is often more: Applied inverse problems using hp-forward models. *Journal of Computational Physics*, 399:108949, 2019.
- [47] C. Sun and J. Liu. An inverse source problem for distributed order time-fractional diffusion equation. *Inverse Problems*, 2020.
- [48] M. Vasilyeva, S. Stepanov, D. Spiridonov, and V. Vasilă-Žev. Multiscale finite element method for heat transfer problem during artificial ground freezing. *Journal of Computational and Applied Mathematics*, 371:112605, 2020.

- [49] A. W. Wharmby and R. L. Bagley. Generalization of a theoretical basis for the application of fractional calculus to viscoelasticity. *Journal of Rheology (1978-present)*, 57(5):1429–1440, 2013.
- [50] Z. Zhang. An undetermined time-dependent coefficient in a fractional diffusion equation. *Inverse Probl. Imaging*, 11(5):875–900, 2017. URL: <https://doi.org/10.3934/ipi.2017041>, doi:10.3934/ipi.2017041.